

Figure S1. XRPD patterns of VLM and multi-component solids.

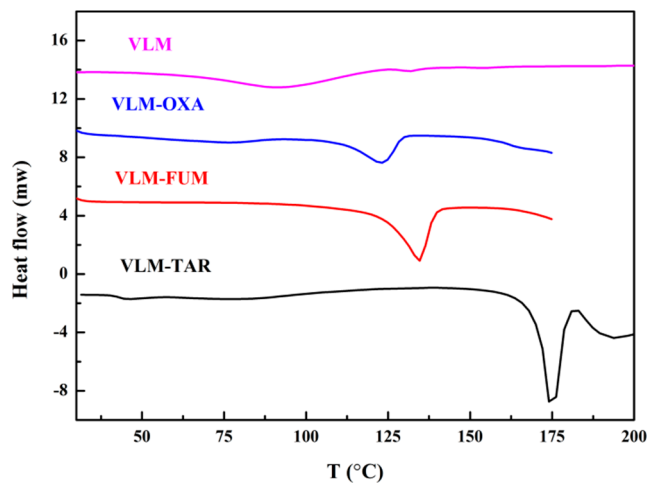


Figure S2. DSC curves of VLM and multi-component solids.

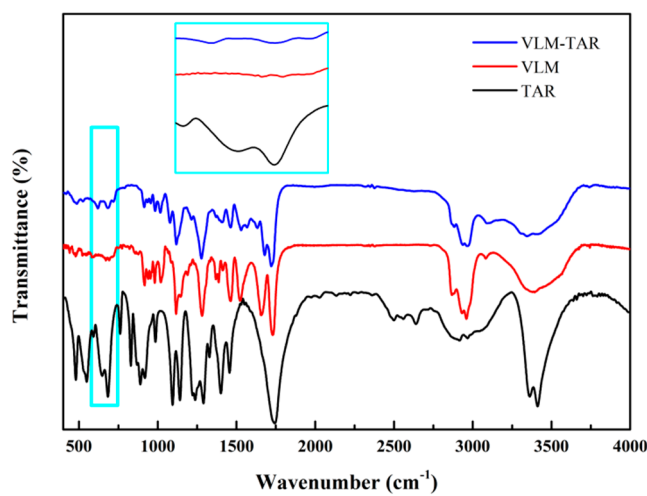


Figure S3. FT-IR spectra of VLM and VLM-TAR multi-component form (inset shows the local amplification of a certain region).

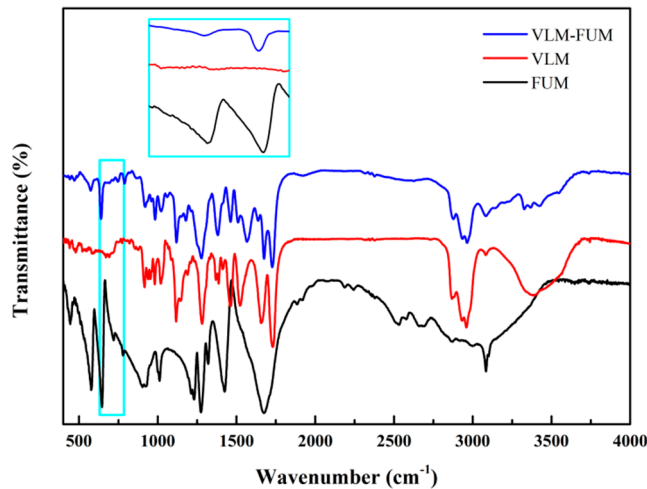


Figure S4. FT-IR spectra of VLM and VLM-FUM multi-component form (inset shows the local amplification of a certain region).

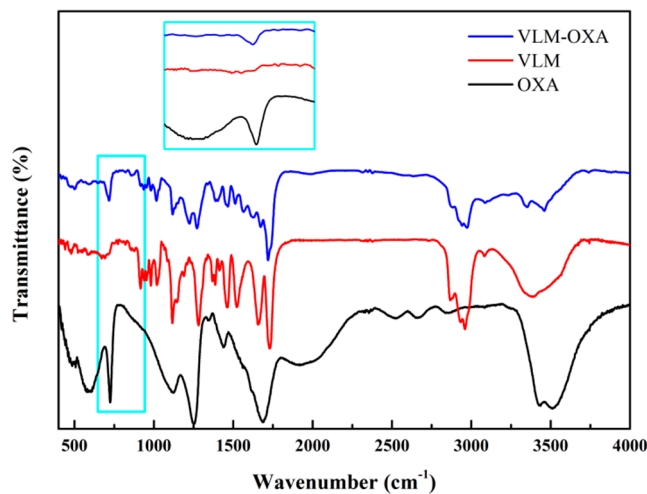


Figure S5. FT-IR spectra of VLM and VLM-OXA multi-component form (inset shows the local amplification of a certain region).

Table S1. Dynamic vapor sorption data for VLM and its multi-component solid forms at 25 °C.

RH (%)	Mass Change (%)			
	VLM	VLM-TAR	VLM-FUM	VLM-OXA
0	0	0	0	0
10	0.38224	0.68945	0.05431	0.41234
20	1.13764	1.02534	0.15198	0.80495
30	1.71855	1.47255	0.2297	1.04885
40	2.26914	1.75625	0.32287	1.2847
50	2.93248	1.91598	0.41114	1.49481
60	4.10728	2.06981	0.5321	1.74609
70	6.43104	2.26723	0.65212	2.14076
80	9.32552	2.50939	1.03933	3.66817
90	14.06428	2.93775	1.62575	4.34447

Table S2. The intrinsic dissolution rate of VLM and its multi-component solid forms in pH = 6.8 aqueous medium at 37 °C.

Time (min)	Concentration (mg/L)				Cumulative Amount (%)			
	VLM	VLM-TAR	VLM-FUM	VLM-OXA	VLM	VLM-TAR	VLM-FUM	VLM-OXA
0	0	0	0	0	0	0	0	0
10	10.13	39.31	45.64	67.86	4.56	17.69	20.54	30.54
20	12.21	65.24	78.85	99.24	5.49	29.36	35.48	44.66
30	13.34	82.46	100.67	126.56	6.00	37.11	45.30	56.95
40	14.37	95.18	112.98	152.77	6.47	42.83	50.84	68.75
50	15.78	100.45	120.96	172.93	7.10	45.20	54.43	77.82
60	17.12	107.20	126.94	182.37	7.70	48.24	57.12	82.07
70	17.56	114.76	130.82	188.34	7.90	51.64	58.87	84.75
80	18.97	123.83	135.52	193.58	8.54	55.72	60.98	87.11
90	19.23	125.82	141.84	200.29	8.65	56.62	63.83	90.13
100	22.35	126.24	145.45	205.85	10.06	56.81	65.45	92.63